SUPPLEMENTARY MATERIALS & METHODS

Animal model

All animal studies were conducted in accordance with NIH guidelines and approved Beth Israel Deaconess Medical Center (BIDMC) Institutional Animal Care and Use Committee IACUC protocol #072-2012. Diabetes was induced in C57BL/6J mice with low doses of streptozotocin (STZ, 50 mg/kg, intraperitoneally) administered for 5 consecutive days, 8 weeks prior to wound healing experiments. Hyperglycemia was confirmed by a fasting blood glucose level exceeding 250 mg/dL. Mice were anesthetized (100 mg/kg ketamine, 5 mg/kg xylazine, intraperitoneally), and full-thickness excisional wounds (6-mm diameter) were produced on the shaved dorsum of the mice. At Days 3 or 10 post-wounding, the surrounding wounded tissue was excised for imaging and stored at -80°C prior to imaging.

Multiphoton microscopy

Unfixed, unstained frozen sections (10μm thickness) from both diabetic and non-diabetic mice were thawed prior to TPEF/SHG imaging. Sections from Day 0 (excised tissue from the punch biopsy), as well as Days 3 and 10 post-wounding, were imaged (512 x 512 pixels; 12-bit depth) with a particular emphasis along the wound edge using a 20x objective (0.7 NA) and a laser-scanning confocal microscope (Leica TCS SP2) equipped with a tunable (710-920 nm) titanium-sapphire laser (Mai Tai; Spectra Physics; Mountain View, CA). To identify collagen fiber deposition, SHG signal using 800nm excitation light was collected in the forward direction by a non-descanned photomultiplier tube (PMT) detector with a 400(±10) nm filter. TPEF signal in the epi-direction was also simultaneously measured by two non-descanned PMTs outfitted with a filter cube that included a 700nm short pass filter and a 495nm dichroic mirror. To isolate

NADH fluorescence using 755nm excitation, a 460(±20)nm emission filter was selected, and FAD fluorescence was isolated using 860nm excitation and a 525(±25)nm emission filter. For in vivo imaging of anesthetized mice, images were acquired with a 25x objective (0.9 NA) with all detectors collecting in the epi-direction.

Quantitative image analysis

Image intensities were normalized for gain and laser power as previously described (Quinn *et al.*, 2013). To facilitate a wider field of view of the entire wound edge, images that were acquired from overlapping fields of view were automatically stitched together using a cross-correlation algorithm in Matlab. Composite false-color images of the wound edge were generated by assigning TPEF and SHG normalized image intensities to RGB color channels. Regions of interest (ROI) were manually defined to identify pixels that corresponded to the granulation tissue, the dermis adjacent to the wound, and the epidermis at the wound edge. An optical redox ratio of FAD/(NADH+FAD) fluorescence intensity was computed at each pixel, and average redox ratios were calculated in the epidermis and granulation tissue ROIs.

Histological analysis

Hematoxylin and eosin (H&E) stained sections of the same wounds were evaluated by an experienced pathologist (AK) blinded to experimental conditions. A neutrophil score (1-4) was assigned based on negligible, mild, moderate, or severe accumulation. Spindle cells (fibroblasts and fibrocytes) and blood vessels were counted within the wound and expressed as counts/ mm^2. Epidermal thickness was measured by counting the number of squamous cell layers.

Statistical analysis

To assess significant differences in redox ratio among STZ treatment, tissue regions and time points, multi-factor ANOVAs of ROI-averaged values were run in JMP 8. Post-hoc Tukey HSD tests were used to evaluate differences within effects. Spearman's rho was computed to determine correlations among multi-photon and histological metrics. Significance was defined as $\alpha=0.05$.

SUPPLEMENTARY TABLE

Table S1. Correlation coefficients (Spearman's ρ) among optical and histological data.

	neutrophil score	blood vessels (per mm^2)	Fibroblast/ fibrocyte count in GT (per mm^2)	Thickness (# of squamous cell layers)
epidermis redox ratio	-0.714*	-0.621*	-0.355*	-0.563*
GT redox ratio	0.5639*	-0.608*	-0.684*	-0.671*
GT SHG intensity	-0.335	0.3183	0.6393*	0.6995*

* $p<0.05$

SUPPLEMENTARY FIGURES

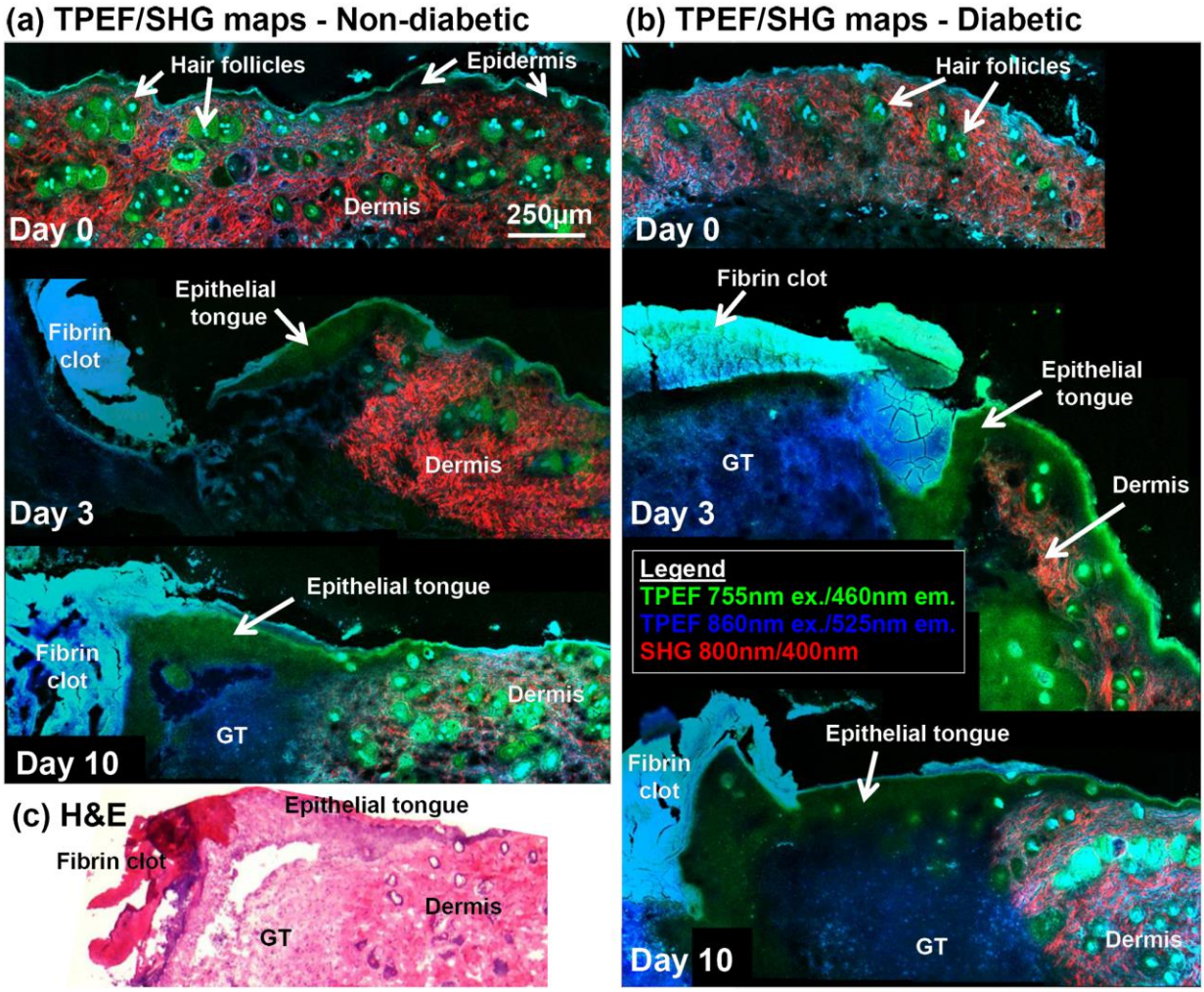

Supplementary Figure 1. An overlay of TPEF and SHG intensity maps of (**a**) non-diabetic and (**b**) diabetic unwounded skin (Day 0) and Day-3 or Day-10 wounds demonstrate an ability to distinguish different tissue features and wound regions similar to hematoxylin and eosin (H&E) staining (c). Collagen SHG is very strong in the adjacent intact dermis, providing a clear distinction between the dermis and granulation tissue (GT). Scale bar in (a) applies to all panels.

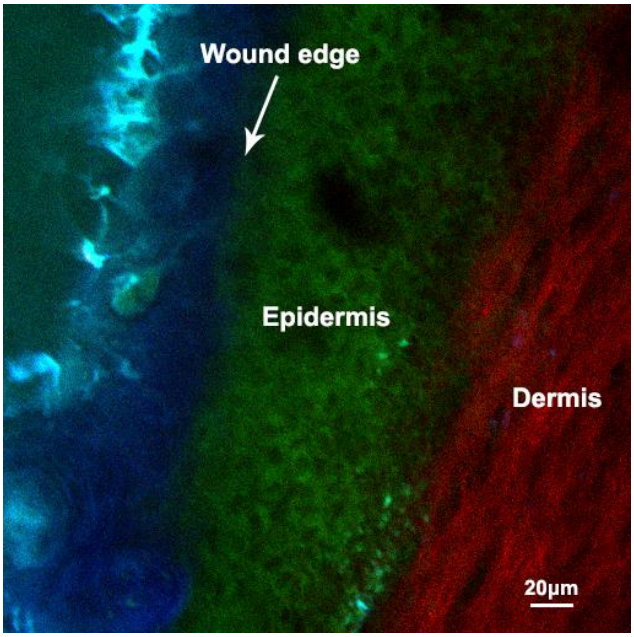

Supplementary Figure 2. Optical section of the wound edge obtained from a live mouse 14 days after wounding, which demonstrates an ability to resolve collagen SHG from the dermis (red), NADH autofluorescence from individual keratinocytes (green), and autofluorescence from the fibrin clot (blue). In contrast to imaging unstained tissue sections of the wound, in vivo images were collected in an *en face* configuration, with the objective relatively perpendicular to the skin surface. The inherent depth sectioning available through multiphoton microscopy enabled the collection of this optical plane which spanned both the surface of the wound, the hyperproliferative epidermis, and the adjacent dermis.